EAI Endorsed Transactions
on Energy Web
Research Article EAI.EU

AC/DC Superimposed Breakdown Characteristics and Electric Field Simulation Analysis of Oil-Paper Insulation in Converter Transformers

Xiaofan Huang*, Jun Yan, Aiqiang Pan and Yufan Zhang

Electric Power Research Institute, State Grid Shanghai Municipal Electric Power Company, Shanghai 200122, China

Abstract

This study investigates the electric field distribution and breakdown characteristics of oil-paper insulation in a 500 kV converter transformer under AC/DC superimposed voltages. The electric field distribution within the winding end insulation structure at the valve side was analyzed under various voltage conditions using finite element simulations. Experiments were conducted on insulating oil and oil-paper samples to measure their breakdown strengths under different AC/DC components. The results reveal that under DC voltage, the electric field concentrates inside the insulation paper, whereas under AC voltage, it is mainly distributed across the oil gap. Under AC/DC superimposed voltages, a decreasing AC ratio shifts the electric field from the oil gap to the insulation paper and increases the maximum electric field strength. As the DC component rises, the breakdown strength of both oil and oil-paper samples first decreases and then increases, with oil-paper insulation consistently exhibiting higher strength. These findings indicate that although oil-paper insulation can withstand higher electric fields and thus ensure transformer safety, low DC components may increase the risk of oil discharge or failure. Therefore, the design of next-generation high-voltage converter transformers must account for oil-paper insulation degradation under low DC ratios, and effective mitigation strategies—such as controlling the internal electric field or enhancing dielectric strength—are essential for ensuring reliability under AC/DC superimposed voltages.

Keywords: Oil-Paper Insulation, AC/DC Superimposed Voltage, Finite Element Method, Electric Field, Breakdown Strength

Received on 24 July 2025, accepted on 15 September 2025, published on 09 February 2026

doi: 10.4108/ew.11840

1. Introduction

Converter transformers are crucial components in power systems, particularly in AC-DC hybrid transmission systems, where they facilitate the conversion of electrical energy between AC and DC systems [1, 2]. In high-voltage direct current (HVDC) power systems, the converter transformers are integral to the converter units, connecting the AC side of the grid to the DC side. Oil-paper insulation, the primary dielectric material used in these transformers, is simultaneously subjected to both AC and DC voltages, resulting in a combined voltage stress. This superimposed voltage stress significantly affects the electrical breakdown properties of the oil-paper insulation. The distribution of the electric field plays a critical role in the breakdown process, as areas with high electric field concentration—often at weak insulation points—are more prone to breakdown [3]. Prolonged exposure to AC/DC superimposed voltage can lead to a shift in the electric field distribution, causing it to concentrate more in the insulation paper. This increased field intensity at weak points can accelerate degradation, resulting in partial discharge, insulation breakdown, or even catastrophic failure, compromising the stability and of reliability HVDC power systems [4, 5]. Therefore, understanding the electric field distribution and its effect on the breakdown behavior of oil-paper insulation under the AC/DC superimposed voltage stress is essential for ensuring

*Corresponding author. Email: xiaofanhuang123@163.com

the long-term performance and safety of converter transformers.

Key parameters such as the dielectric strength and loss of oil-paper composite insulation, which are decisive for system reliability, are highly sensitive to variations in moisture concentration and aging condition. As established in prior studies, the presence of these factors is known to elevate the system's dielectric loss [6]. Furthermore, extended thermal aging induces deterioration in breakdown characteristics, resulting in a stress-life relationship that quantifies the significant reduction in electrical endurance [7]. Research on material improvements has shown that mixed insulating oils promote a higher degree of polymerization in paper compared to mineral oil, thereby enhancing transformer anti-aging capabilities [8]. This benefit is quantitatively supported by findings that vegetable oil effectively attenuates the degradation rate of paper, thus prolonging its functional service life [9].

Space charge, partial discharge, and breakdown characteristics serve as critical proxies for assessing the condition and performance of oil-paper insulation systems. Research indicates that space charge behavior is severely influenced by factors including impulse voltage, temperature, and moisture. Furthermore, thermal aging markedly intensifies space charge accumulation dynamics, leading to significant charge build-up throughout the bulk of the oil-paper insulation and at its interfacial surfaces [10]. Further studies on partial discharge patterns revealed a noteworthy escalation in both the magnitude and frequency of discharges with extended thermal aging [11]. In addition, a model of breakdown characteristics was developed under combined AC-DC voltages, taking into account different stages of thermal aging. A consistent deterioration of breakdown voltage was observed in the model with rising temperature and prolonged thermal aging [12]. Among various electrical parameters, breakdown strength serves as a critical indicator for directly and reliably evaluating the functional state of insulation systems [13].

The dielectric strength of insulation materials under electrical stress is a key parameter for assessing their performance. Investigations into oil-paper insulation have revealed that various factors influence its breakdown behavior. As early as 1976, it was observed that under AC–DC superimposed voltage conditions, the AC component exerts a more pronounced influence on the breakdown strength of oil-paper insulation than the DC component [14]. Subsequent work confirmed that moisture reduces the dielectric strength of oil-paper insulation in composite electric fields [15]. Further research demonstrated that enlarging the oil gap leads to a decline in breakdown strength under both AC and DC voltages [16]. Electrical aging studies have also shown that increased temperature lowers the short-term withstand voltage of oil-paper insulation under pulsating DC stress [17]. Moreover, research involving superimposed harmonic components indicates that higher harmonic levels accelerate insulation deterioration, with higher-order harmonics exerting a stronger effect on reducing breakdown time than lower-order ones [18]. Collectively, these studies highlight the critical roles of voltage waveform, moisture, temperature, and harmonic distortion in determining the breakdown characteristics and service life of oil-paper insulation.

In this study, the breakdown characteristics and electric field distributions of the oil-paper insulation in a 500 kV converter transformer are investigated under the AC/DC superimposed voltages. Finite element simulations were conducted to analyze the electric field distributions under various voltage conditions, with a focus on the impact of both AC and DC components. The study also includes experimental tests on insulating oil and oil-paper insulation samples to evaluate their breakdown strength under the AC/DC superimposed voltages with different AC/DC voltage ratios. The results provide valuable insights into the insulation performance and the interaction between AC and DC voltages, offering theoretical guidance for optimizing the insulation design of converter transformers in complex electrical environments.

2. Material Preparation And Experimental Details

2.1. Material Preparation

The oil samples and oil-paper insulation samples were collected from a 500 kV converter transformer, with the insulation paper having an approximate thickness of 0.2 mm. Prior to the experiments, the insulation paper samples were immersed in #25 transformer oil for 24 hours under vacuum conditions to prepare the oil-paper insulation specimens and replicate their operational environment. The breakdown tests were repeatedly performed 12 times under the identical DC preload voltage conditions to ensure the accuracy and reproducibility of the experimental results.

2.2. Experimental Setup

The custom-designed AC/DC superimposed breakdown platform, as shown in Figure 1, is used to conduct breakdown testing on the oil-paper insulation samples. These samples are immersed in No. 25 transformer oil to effectively prevent surface flashover. To isolate the effects of DC voltage on the AC sources, a DC-isolated capacitor and a DC-isolated resistor are employed, while an AC-isolated resistor is used to mitigate the influence of AC voltage on the DC sources. Specifically, the components have the following values: 0.1 μF for the DC-isolated capacitor, 10 MΩ for the DC-isolated resistor, and 1 MΩ for the AC-isolated resistor. The superimposed AC and DC voltages are applied to the spherical electrode positioned above the sample. Meanwhile, the lower side of the sample is in contact with another spherical electrode, which is grounded. The combined AC and DC voltages are measured using a voltage divider circuit. This experimental setup allows for precise testing of the breakdown characteristics under both AC and DC stress

conditions, which is essential for understanding the insulation performance in complex electrical environments.

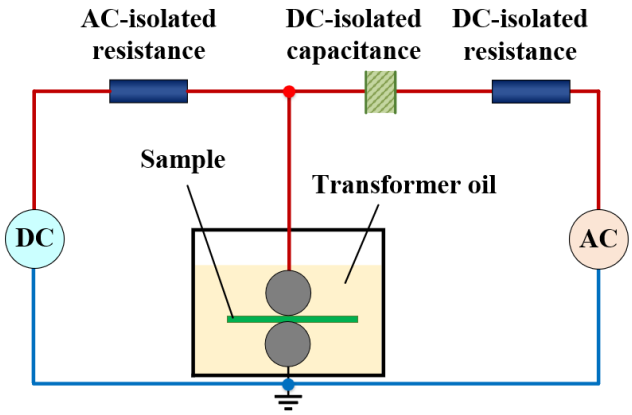

Figure 1. Schematic diagram of AC and DC superimposed breakdown test setup

2.3. Experimental Method

The experimental procedure for investigating the breakdown characteristics of oil-paper insulation under combined electrical stress is schematically represented in Figure 2. The test protocol initiates with a ramping up of the DC voltage at a controlled rate of 0.1 kV/s. Upon reaching the predetermined DC bias level, this voltage is maintained constant for a duration of 30 seconds. This pre-stressing phase is critical for establishing a stable electric field condition within the insulation prior to the application of the AC stress. Subsequently, the AC voltage is introduced and increased at a rate of 0.5 kV/s until the sample undergoes electrical breakdown. The specific voltage values for both the DC and AC components are captured automatically at the instant of failure.

This meticulous methodology is designed to systematically probe the synergistic effects of AC and DC voltages on the insulation's failure mechanism. By precisely controlling the voltage application sequence and rates, the experiment effectively simulates the complex electrical stresses encountered in operational converter transformers. The recorded breakdown data provides a direct measure of the insulation's withstand capability under composite stress, offering critical insights into the interplay between the two voltage components. Furthermore, the integrity of the applied voltage waveform and the testing process is validated by the schematic in Figure 3 and the actual measured waveform presented in Figure 4, respectively. The comprehensive dataset obtained is indispensable for understanding insulation failure thresholds and for developing more accurate life assessment models.

The AC voltage ratio α in the AC/DC superimposed voltage can be calculated using the following formula:

$$\alpha = \frac{U_{\mathrm{ac}}}{U_{\mathrm{dc}}+U_{\mathrm{ac}}} \quad (1)$$

where Uac is the amplitude of the AC voltage and U_{dc} is the amplitude of the DC voltage.

The Weibull distribution is widely used for modeling reliability data. The strength data were analyzed using the two-parameter Weibull distribution, as expressed in formula (2):

$$F(t) = 1 - \exp\left[-\left(\frac{t}{\alpha}\right)^{\beta}\right] \quad (2)$$

where $F(t)$ is the breakdown field strength, α (the scale parameter) indicates the 63.2% breakdown probability threshold, and β (the shape parameter) quantifies the data dispersion.

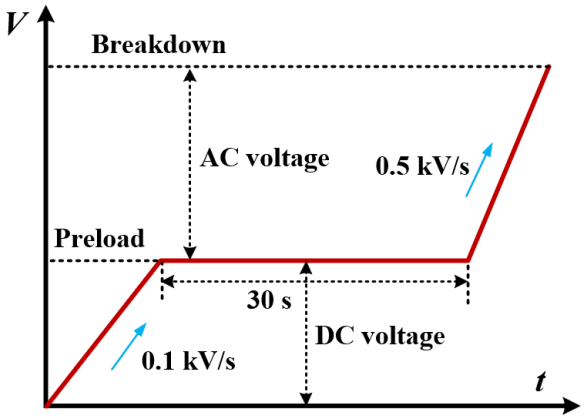

Figure 2. Testing method for AC/DC voltage superposition

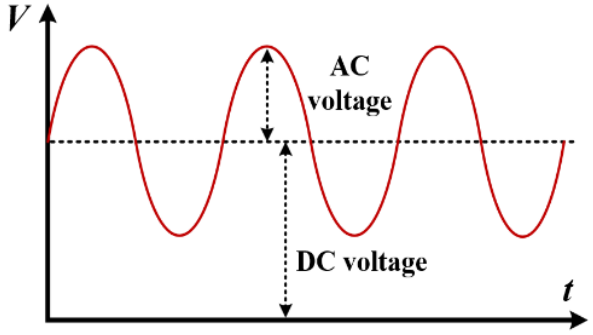

Figure 3. Waveform diagram of the AC/DC superimposed voltage

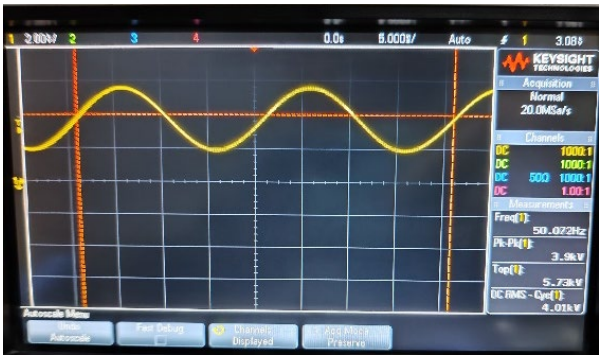

Figure 4. Measured AC/DC superimposed voltage waveform

3. Simulation And Experimental Results

3.1. Electric field Simulation of End of Converter transformer

The valve-side winding end of a converter transformer constitutes a critical insulation region due to its complex geometry and exposure to diverse voltage components. This study investigates the electric field distribution and insulation performance in this region under pure DC, pure AC, and AC/DC superimposed voltages. A finite element model of the winding end was developed using COMSOL Multiphysics to simulate the electric field distributions under these voltage conditions. The results provide theoretical support for the insulation design of converter transformers. As shown in Figure 5, the model geometry includes the valve-side winding and the oil-paper insulation structure. It is used to analyze the effects of pure DC, pure AC, and AC/DC superimposed voltages on the insulation system. In the model, the electrostatic shield is connected to the high-voltage winding, while the outer shell is grounded. The insulation paper is layered, with the interlayer gaps fully impregnated with insulating oil.

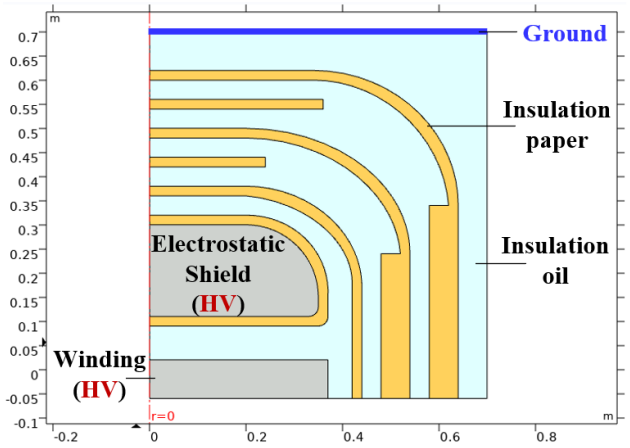

Figure 5. Finite element method model of the end of converter transformer winding

The high voltage applied to the winding and its electrostatic shield is set to 500 kV DC or AC in the simulation. The relative dielectric constants of the insulation paper and the insulating oil are 4 and 2, respectively, while their electrical conductivities are 10^{-13} S/m and 10^{-11} S/m. The DC and AC electric field distributions at the winding end of the converter transformer are shown in Figure 6 and Figure 7, respectively. In addition, the effects of different AC voltage components in the AC/DC superimposed voltage on the transient electric field distribution are investigated. The time ranges from 0 s to 50.005 s, with a time step of 1 s. The transient electric field distributions and the maximum values at the winding end of the converter transformer are recorded at various time intervals.

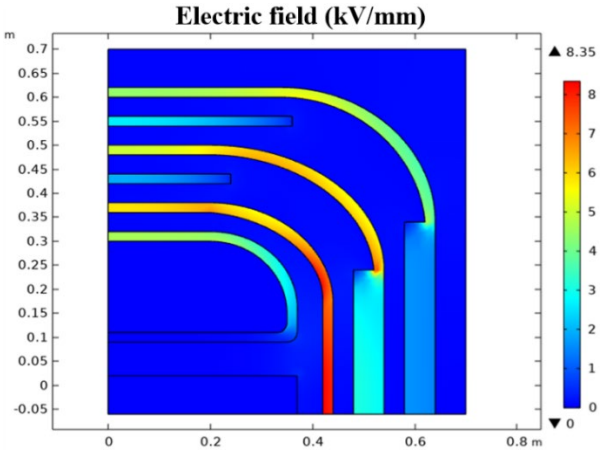

Figure 6. Electric field distribution at the end of converter transformer winding under the DC voltage

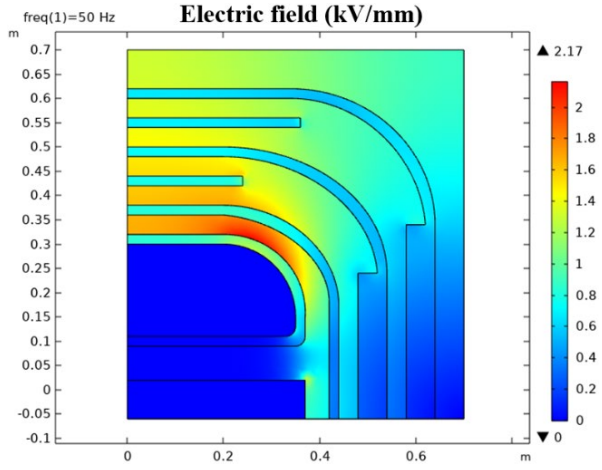

Figure 7. Electric field distribution at the end of converter transformer winding under the AC voltage

The electric field under DC conditions peaks at a significantly higher value of 8.35 kV/mm. In stark contrast, the AC field is largely confined to the oil gap adjacent to the electrostatic ring, reaching a maximum of only 2.17 kV/mm—merely a quarter of the DC peak. This substantial disparity underscores the more demanding electric stress imposed by the DC component. For the valve-side winding, which is inherently subjected to combined AC and DC voltages, the field distribution exhibits a strong dependency on their ratio. Analysis reveals that as the AC component diminishes, the electric field at the winding end undergoes a critical transition, shifting its concentration from the

insulating oil towards the solid insulation paper. This spatial redistribution is accompanied by a continuous and attendant increase in the maximum field strength. The escalation is particularly concerning because solid insulation, such as paper, often has a different dielectric withstand capability compared to oil. Consequently, this elevated and redistributed field drastically raises the threat of initiation and propagation of partial discharges, ultimately leading to the electrical breakdown of the oil-paper insulation system.

When an AC/DC superimposed voltage is applied to the model electrode, with the AC voltage component at 60% (i.e., an AC voltage amplitude of 300 kV and a DC voltage amplitude of 200 kV), the electric field distributions at the winding end of the model at simulation times of 5.005 s and 50.005 s are shown in Figure 8 and Figure 9, respectively.

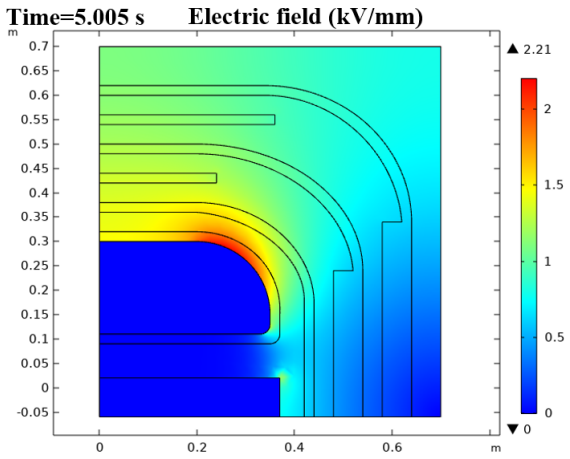

Figure 8. Electric field distribution at the end of converter transformer winding under the AC/DC superimposed voltage at 5.005 s

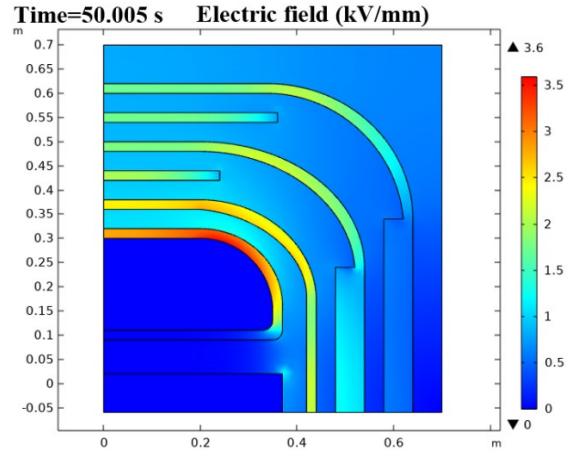

Figure 9. Electric field distribution at the end of converter transformer winding under the AC/DC superimposed voltage at 50.005 s

From Figure 8 and Figure 9, it can be observed that at 5.005 s, the electric field is primarily distributed in the insulation paper and oil gap near the electrostatic shield. At 50.005 s, the electric field is mainly concentrated within the insulation paper, with the field strength increasing closer to the electrostatic shield. The maximum electric field strength increases from 2.2 kV/mm to 3.6 kV/mm. As the simulation time progresses, the high electric field value gradually shifts from the oil gap to the insulation paper.

The simulation model is subjected to a 500 kV AC/DC superimposed voltage to investigate the effects of AC/DC component ratio on the electric field distribution at the converter transformer winding end. Figure 10 shows the evolution of the maximum electric field strength over time for different AC ratios. The maximum electric field value increases with time before stabilizing after approximately 40 s. A clear trend is observed: a lower AC ratio leads to a significantly higher electric field. Specifically, the peak electric field strength is 2.17 kV/mm for a 100% AC ratio, increases to 4.84 kV/mm (over twice the all-AC value) at a 40% AC ratio, and reaches 7.24 kV/mm (nearly three times the all-AC value) under pure DC (0% AC) conditions.

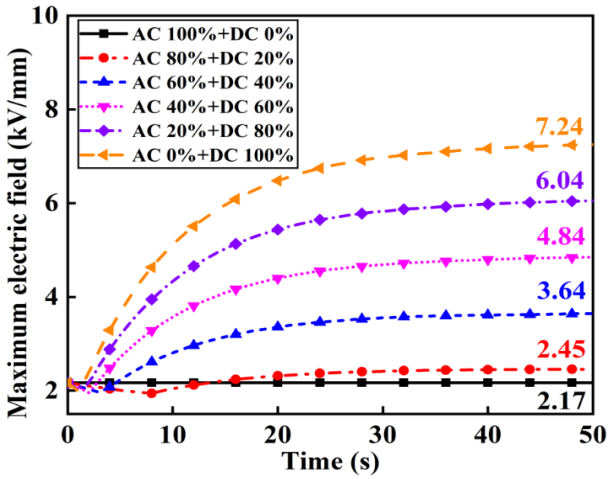

Figure 10. Maximum electric field at the winding end of converter transformer under the AC/DC superimposed voltages with different voltage ratios

3.2. Surface Morphology

The surface morphology of the oil-paper insulation samples after breakdown under AC voltage, DC voltage, and AC/DC superimposed voltage is shown in Figure 11. After AC breakdown, the sample surface shows a small black spot, which is a carbonized channel formed by the cleavage of cellulose molecular chains in the oil-paper insulation. In contrast, after DC breakdown, the surface exhibits a through-hole, with black carbon deposits on the hole walls. When the sample undergoes breakdown under AC/DC superimposed voltage, a larger through-hole appears, and a significant area

of carbon traces surrounds the hole. The sample also shows noticeable ablation marks, indicating severe damage caused by the high current generated during the breakdown. This large current generates substantial Joule heat, resulting in extensive damage to the sample. These observations suggest that the combined AC/DC voltage has a more significant destructive effect on the sample, likely due to the higher energy released during breakdown.

Figure 11. Surface morphology of oil paper insulation after breakdown

3.3. Breakdown Characteristics of Oil-paper Insulation

The AC breakdown voltages of the oil-insulation paper samples under different DC preloads (0-7 kV) and the DC breakdown voltages are presented in Table 1 and Table 2. According to formula (2), the Weibull statistics distributions of the AC breakdown strengths of the oil-insulation paper samples under different DC preloads (0-7 kV) and the DC breakdown strengths are calculated and presented in Figure 12 and Figure 13. As shown in Figure 12, when the DC preset voltage increases from 0 kV to 4 kV, the AC breakdown field strength gradually decreases. This suggests that the presence of DC voltage, even at low levels, negatively impacts the insulation's ability to withstand AC voltage stress. The reduction in breakdown strength could be attributed to the cumulative stress of the superimposed AC and DC voltages, which causes greater polarization effects and enhances the degradation of the insulation material.

Figure 13 provides further insights into the behavior of the AC breakdown field strength when subjected to higher DC preloads. As the DC preset voltage increases from 5 kV to 7 kV, an interesting pattern emerges: the AC breakdown field strength of the oil-insulation paper samples initially increases before declining. The maximum AC breakdown field strength occurs at a DC preset voltage of 6 kV, indicating that, within this specific range, the applied DC voltage may create favorable conditions for the AC stress to be more effectively withstood. This could be due to the interaction between the DC voltage and the AC electric field, which modifies the breakdown mechanism by altering the local electric field distribution or reducing the effect of surface conductivity, leading to improved insulation performance at a certain DC voltage level.

From the overall analysis of these results, it can be concluded that the DC breakdown field strength is consistently greater than the AC breakdown field strength across all tested voltage levels. This aligns with the common understanding that DC voltage tends to exert more stable and predictable stress on insulation compared to AC voltage, due to the absence of voltage reversals in DC. Furthermore, when a DC preset voltage is applied, it leads to a reduction in the AC breakdown field strength. This reduction is likely due to the combined effect of AC and DC voltages, which may cause synergistic degradation of the insulation material. The presence of DC voltage can alter the charge distribution and cause polarization effects that weaken the insulation, making it more susceptible to breakdown under AC stress. These findings underscore the importance of considering both AC and DC voltage stresses in evaluating the performance and reliability of insulation materials. The interaction between AC and DC voltages can significantly impact the insulation's long-term durability, and further studies are needed to better understand the underlying mechanisms and optimize insulation materials for such conditions.

Table 1. AC breakdown voltages of the oil-paper samples under different DC preloads (0-4 kV)

DC 0 KV	DC 1 KV	DC 2KV	DC 3 KV	DC 4KV
7.45	5.88	4.85	3.90	3.23
7.43	5.23	4.35	3.70	3.45
7.52	5.30	4.30	4.00	3.55
7.41	5.52	4.55	3.95	2.98
7.48	5.34	4.65	4.10	3.00
7.58	5.45	4.45	3.80	3.15
7.67	5.25	4.60	3.95	3.30
7.24	5.49	4.375	4.05	3.35
7.36	5.62	4.55	3.80	3.05
7.59	5.71	4.62	3.75	3.20
7.36	5.69	4.50	4.05	3.42
7.55	5.58	4.73	3.73	3.50

Table 2. AC breakdown voltages of the oil-paper samples under different DC preloads (5-7 kV) and the pure DC breakdown voltages

DC 5 KV	DC 6 KV	DC 7 KV	Pure DC
2.38	3.23	2.87	9.30
2.10	3.15	2.78	9.05
2.92	3.74	2.87	9.51
2.50	3.55	2.55	9.22
2.55	3.45	2.65	9.45

2.46	3.33	2.84	9.50
2.25	3.64	2.65	9.16
2.78	3.35	2.82	9.34
2.36	3.28	2.55	9.63
2.54	3.66	2.69	9.44
2.22	3.58	2.56	9.38
2.67	3.51	2.65	9.25

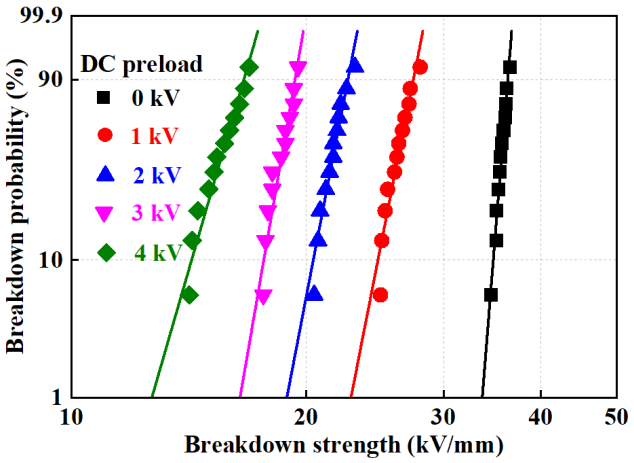

Figure 12. Weibull distributions of AC breakdown strengths of the oil-paper samples under different DC preloads (DC 0-4 kV)

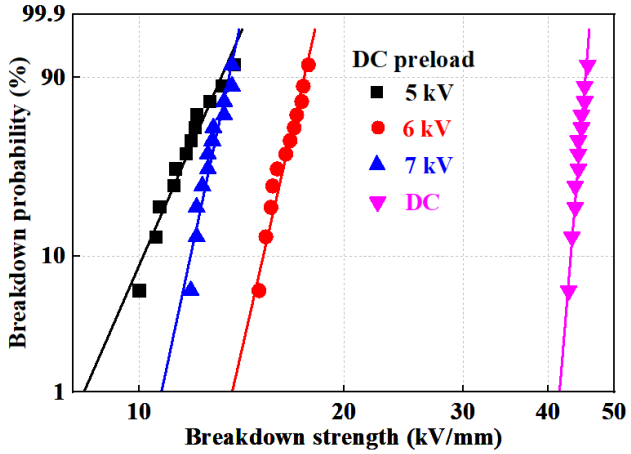

Figure 13. Weibull distributions of AC breakdown strengths under different DC preloads (5-7 kV) and DC breakdown strengths of the oil-paper samples

The AC/DC superimposed breakdown field strengths of the insulating oil and oil-paper insulation under different DC voltage presets are shown in Figure 14 and Figure 15, respectively. As the DC voltage ratio increases, the AC/DC breakdown field strength of both insulating oil and oil-paper insulation initially decreases and then increases. Additionally, the AC/DC breakdown field strength of oil-paper insulation is significantly higher than that of insulating oil. According to the simulation results, as the DC component increases, the electric field becomes more concentrated within the oil-paper insulation, with the maximum field strength gradually increasing. However, oil-paper insulation can withstand higher electric fields than insulating oil, ensuring the safe and reliable operation of the converter transformer's insulation system. Notably, a lower DC component leads to a decrease in the breakdown field strength, during which the insulating oil predominantly bears the electric field of the winding insulation structure, potentially leading to the risk of discharge or failure in the insulating oil.

At lower DC voltage components, the injection of a small amount of space charges into the oil-paper insulation distorts the internal electric field and can induce partial discharge, ultimately degrading the breakdown strength under combined AC/DC stress. Conversely, a higher DC component drives more space charges to migrate toward the hetero-electrode in the oil-paper insulation. This migration weakens the internal field, thereby unexpectedly enhancing the AC/DC superimposed breakdown strength.

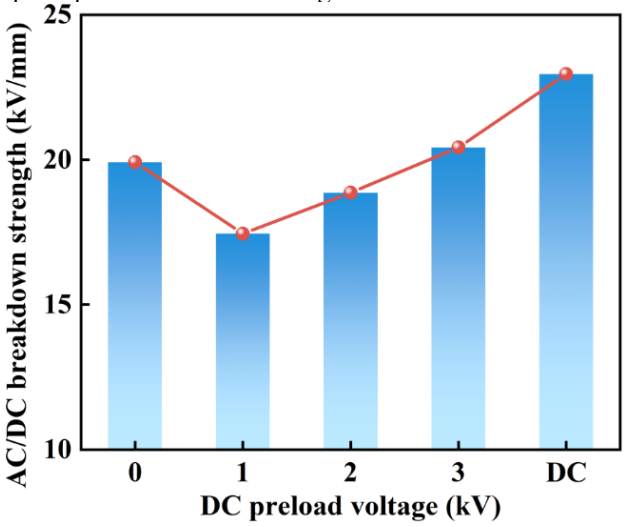

Figure 14. AC/DC superimposed breakdown strength of the oil samples

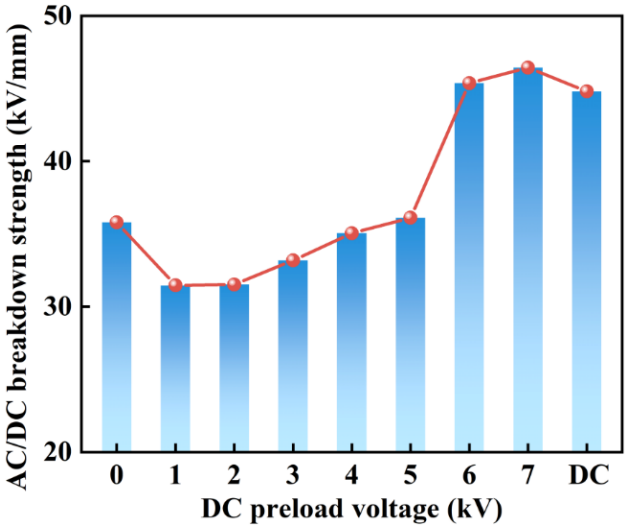

Figure 15. AC/DC superimposed breakdown strength of the oil-paper samples

4. Conclusion

This study, based on finite element method simulations, investigates the electric field distribution at the winding end insulation structure of a 500 kV converter transformer under AC/DC superimposed voltage. Additionally, experimental tests were conducted to obtain the AC/DC superimposed breakdown field strength of insulating oil and oil-paper insulation samples under varying DC components. The main conclusions are as follows:

Finite element simulations reveal that the electric field concentrates within the insulation paper under DC voltage, with a more intense field near the electrostatic shield. Under AC voltage, the electric field is primarily focused in the oil gap, and the maximum field strength is significantly lower than under DC. When an AC/DC superimposed voltage is applied, a decrease in the AC component leads to a gradual increase in the maximum electric field and a shift in the field concentration from the oil gap to the insulation paper.

Experimental tests reveal that as the DC component increases, the AC/DC superimposed breakdown strength first decreases and then increases. The oil-paper insulation has a significantly higher breakdown strength than the insulating oil. The study highlights that oil-paper insulation can withstand higher electric fields than insulating oil, ensuring transformer safety. However, lower DC components may reduce superimposed breakdown strength, increasing the risk of oil discharge or failure.

Future converter transformer designs must address the detrimental impact of DC voltage components on oil-paper insulation, as a low DC content in AC/DC superimposed voltages reduces its breakdown strength and increases the maximum electric field. To mitigate the electric field concentration in the insulation paper, strategies are needed to reduce the internal electric field intensity. Practical pathways to achieve this include increasing the paper's layers or thickness, or directly improving its dielectric strength through chemical modification.

Acknowledgements.

This word was supported by the State Grid Shanghai Municipal Electric Power Company program (Study on Probability Modeling of Extreme Disaster Events Considering Tail Risk and Its Application in Urban Power Grid Resilience Assessment, Grant No. 52094024001C).

References

[1] Qian G, Dai X, Shi S, et al. Electric Field-Dependent XY Equivalent Structure Modeling of Oil-Paper Insulation Systems in Power Transformers: Improvement and Verification[J]. IEEE Transactions on Dielectrics and Electrical Insulation, 2025, 32(5): 2986-2994.

[2] Gong H, Liu J, Jiang Z et al. A Time-Domain Fractional Element Model for Aging Condition Analysis of Hot-Spot Region Insulation in Power Transformer[J]. IEEE Transactions on Instrumentation and Measurement, 2024, 73: 1–11.

[3] P. Ghosh, B. Chakraborty, B. Chatterjee, S. Dalai and S. Chatterjee. Investigations on the Impact of Paper Moisture on Nanoparticles Dispersed Oil-Paper Insulation Using Lightning Impulse Parameters[J]. IEEE Transactions on Plasma Science, 2025, 53(6): 1324-1332.

[4] Zuo K, Shen W, Cui H, et al. The Breakdown Characteristics of Oil-Paper Insulation in Converter Transformers[C]. International Symposium on Electrical Insulating Materials (ISEIM), 2020: 537-540.

[5] Zhou G, Wang Q, Shi Y, et al. Research on Deterioration Mechanism of Oil-paper Insulation of 220 kV Current Transformer[C]. IEEE 5th Conference on Energy Internet and Energy System Integration (EI2), 2021: 3744-3749.

[6] Gao S, Lei Y, Liu Y, et al. The Corrosion and Activation Mechanism of Thiophenic Sulfides in the Oil-Paper Insulation[J]. IEEE Transactions on Dielectrics and Electrical Insulation, 2025, 32(3): 1353-1363.

[7] Qin F, Li S, Chen Z, et al. Breakdown Characteristics and Damage Mechanism of Typical Defects in Oil-Paper Insulation Under HEMP[J]. IEEE Transactions on Dielectrics and Electrical Insulation, 2025, 32(2): 1046-1055.

[8] Yang C, Zhao T, Liu Y, et al. Partial Discharge and Deterioration Characteristics of Oil-Immersed Pressboard Under Bubble Defects[J]. IEEE Transactions on Dielectrics and Electrical Insulation, 2024, 31(6): 3453-3461.

[9] Zhang H, Liu J, et al. Aging Assessment of Insulating Paper Based on Furfural Concentration Prediction in Transformer Oil[J]. IEEE Transactions on Dielectrics and Electrical Insulation, 2024, 31(4): 2226-2234.

[10] A. Kumar, D. Mishra and A. Baral. Importance of Depolarization Current in the Diagnosis of Oil-Paper Insulation of Power Transformer[J]. IEEE Access, 2023, 11: 56858-56864.

[11] Fubao J and Yuanxiang Z. Effect of Electric-Field Components on the Flashover Characteristics of Oil-Paper Insulation Under Combined AC-DC Voltage[J]. IEEE Access, 2023, 11: 556-563.

[12] H. H. Goh, Yin J, Zhang Y. Study on Lifespan Prediction of Oil–Paper Bushing Considering the Influence of Moisture-Accelerated Aging[J]. IEEE Transactions on Dielectrics and Electrical Insulation, 2023, 30(1): 458-465.

[13] P. Ghosh, B. Chakraborty, B. Chatterjee, et al. An Advanced Technique for Investigating the Moisture Effect on Next Generation Transformer Insulation Using Lightning Impulse Parameters[J]. IEEE Transactions on Plasma Science, 2024, 52(5): 1739-1746.

[14] A. A. Devadiga and S. H. Jayaram. Effects of Repetitive Fast Transients on Aging of Transformer Insulation[J]. IEEE Transactions on Dielectrics and Electrical Insulation, 2024, 31(4): 2189-2197.

[15] Chen G, Xin X, Luo L, et al. Numerical Simulation of Multibranching Positive and Negative Streamer Discharges Near the Oil-Paper Interface in Dielectric Liquid During Pulsed Voltage[J]. IEEE Transactions on Dielectrics and Electrical Insulation, 2024, 31(4): 1981-1987.

[16] Zhao T, Liu Y, et al. Bubble Motion Characteristics in the Transformer Oil Gap at the Top of HV Winding[J]. IEEE Transactions on Dielectrics and Electrical Insulation, 2024, 31(6): 3360-3367.

[17] Zheng Z, Lu B, Gan W, et al. Aging Characterization of Oil-Paper Insulation Based on Fluorescence Characteristics of

Suspended Fibers in Oil[J]. IEEE Transactions on Dielectrics and Electrical Insulation, 2024, 31(6): 3405-3413.

[18] S. K. Ojha, P. Purkait and S. Chakravorti. Evaluating the Effects of Temperature on Moisture Dynamics and Relaxation Mechanism in Transformer Oil-Paper Insulation[J]. IEEE Transactions on Dielectrics and Electrical Insulation, 2024, 31(1): 151-159.